



**Immobilizing proteins on silica with site-specifically  
attached modified silaffin peptides**

Journal:	<i>Biomaterials Science</i>
Manuscript ID:	BM-ART-08-2014-000310.R1
Article Type:	Paper
Date Submitted by the Author:	15-Oct-2014
Complete List of Authors:	Lechner, Carolin; University of Vienna, Chemistry Becker, Christian; University of Vienna, Chemistry

Cite this: DOI: 10.1039/c0xx00000x

www.rsc.org/xxxxxx

ARTICLE TYPE

# Immobilising proteins on silica with site-specifically attached modified silaffin peptides†

Carolyn C. Lechner<sup>a,b</sup> and Christian F.W. Becker<sup>\*a</sup>

Received (in XXX, XXX) Xth XXXXXXXXX 20XX, Accepted Xth XXXXXXXXX 20XX

DOI: 10.1039/b000000x

Immobilisation of proteins on solid supports such as silica is commonly applied to improve performance of enzymes under detrimental conditions and to allow enzyme recycling. Silica biomineralisation processes occurring in nature have recently inspired approaches towards mild, biomimetic silica formation. In diatoms, complex posttranslationally modified silaffin peptides are directly involved in formation and patterning of silica cell walls. Here, chemically modified silaffin peptides are used to establish a novel strategy for silica immobilisation of target proteins. Silaffin variants carrying different modifications are covalently linked to eGFP and thioredoxin using expressed protein ligation. Covalent eGFP- and thioredoxin-silaffin conjugates are able to efficiently precipitate silica and control silica properties by choice of different silaffin modifications leading to functional encapsulation of these proteins in silica particles. Covalent protein-silaffin conjugates lead to a distinctly more efficient and homogenous encapsulation of proteins in silica, superior to random protein entrapment resulting from simple co-precipitation. Silica-immobilised proteins are confirmed to be fully active and stabilised against denaturation.

## Introduction

The immobilisation of functional biomolecules, such as enzymes is beneficial for diverse biotechnological and medicinal applications due to improved properties of the immobilised biomolecules. In the case of enzymes, immobilisation can improve stability and activity under detrimental reaction conditions or enable recycling of these sensitive biomolecules.<sup>1</sup> These effects can be achieved by linking enzymes to a solid support, either via covalent bonds or physical adsorption, by encapsulating them or by cross-linking enzymes into large aggregates.<sup>2</sup> For immobilisation or encapsulation of enzymes, mesoporous silica materials have gained substantial attention as support matrix due to their convenient properties. This material provides a large surface area with uniform pore sizes, the surface silanol groups can be easily functionalised and silica has a high chemical and physical stability. Mesoporous silica nanoparticles (MSNs) are synthesised using an organic template that is removed after silica formation,<sup>3</sup> allowing the control of silica morphology and pore sizes by choosing suitable templating molecules and reaction conditions.<sup>4,5</sup> However, the efficiency in loading of mesoporous silica materials via adsorption of an enzyme turned out to be also dependent on protein size and properties.<sup>6</sup> This inefficient and slow process, in combination with the elaborate syntheses of MSNs under harsh conditions are major drawbacks of synthetic silica materials as solid support for enzyme immobilisation. In contrast, biogenic formation of silica materials occurs under mild, physiological conditions and takes place in diatoms,

sponges and higher plants.<sup>7</sup> Eukaryotic, unicellular diatoms are major producers of amorphous silica in aqueous habitats and have remarkably nano-structured, porous frustules composed of amorphous silica and organic matter.<sup>7</sup> Due to its highly regular, porous structure with a large surface area, diatom silica is a convenient carrier for proteins. The porous silica frustules can be modified or loaded with biomolecules and thus be used in biotechnological and biomedical approaches such as immunoprecipitation, biosensing and drug delivery.<sup>8-12</sup>

The molecular mechanisms of silica biogenesis in diatoms were extensively investigated to gain insights into these complex processes and to establish novel routes for generating structured silica materials under mild conditions. The chemical analysis of diatom cell walls led to the discovery of numerous biomolecules, including polysaccharides,<sup>13</sup> long chain polyamines (LCPAs)<sup>14,15</sup> and several proteins,<sup>16-22</sup> including silaffins,<sup>23</sup> that are associated with diatom biosilica. Silaffins and LCPAs are directly involved in the silica precipitation process *in vivo* and have also been shown to precipitate silica from a solution of silicic acid *in vitro*.<sup>14,23</sup> Silaffin peptides from the diatom *C. fusiformis* derive from proteolytic processing of a precursor polypeptide comprising repetitive units.<sup>23</sup> During maturation silaffin peptides become extensively posttranslationally modified. The numerous serine hydroxyl groups are phosphorylated and the  $\epsilon$ -amino groups of lysine residues become di- or trimethylated or alkylated with long-chain polyamines.<sup>24,25</sup> Additionally, hydroxylation and phosphorylation of the trimethylated lysine residues at the  $\delta$ -position was observed.<sup>25</sup> Although these posttranslational modifications (PTMs) turned out to be essential for silica

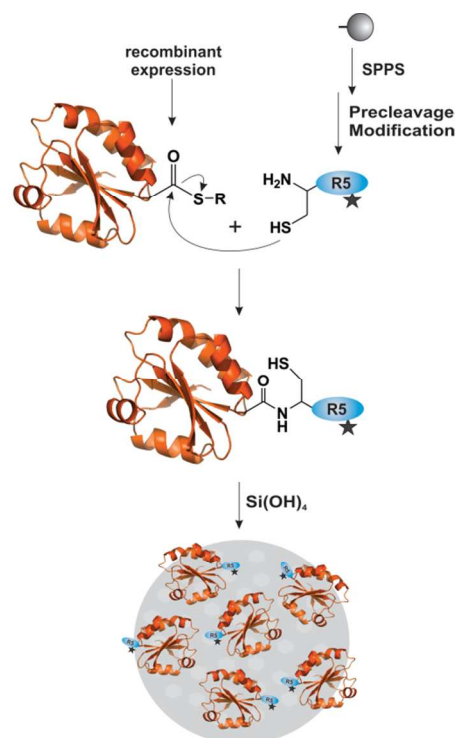
precipitating activity under native conditions (pH 5)<sup>23</sup> a synthetic silaffin R5 peptide without any modification (SSKKSYSYSGSKGSKRRIL) is also highly efficient in precipitating silica from a solution of silicic acid at neutral pH in the presence of phosphate ions.<sup>23-26</sup>

Several strategies for enzyme immobilisation using silaffin peptides as mild silica precipitation agent have been developed. One approach is based on genetic manipulation of diatoms with the sequence of a target protein being genetically fused to a silaffin gene.<sup>27</sup> The fusion protein is produced by the diatom and becomes tightly associated with the newly formed silica frustules during silica biogenesis. The protein-containing biosilica is subsequently purified and the enzymes remain active and are considerably stabilised.<sup>27,28</sup> Fusion proteins comprising a target protein and the R5 sequence can also be obtained by recombinant expression in *E. coli*. However, silaffin tags produced in bacteria lack posttranslational modifications and therefore a major factor that controls silica morphology is missing. Purified protein-silaffin chimeras can be used for *in vitro* silica precipitation resulting in auto-encapsulation of the protein during silica formation.<sup>29-31</sup> In another approach, synthetic silaffin R5 peptides are mixed with a solution of target enzyme without prior covalent linkage. During silaffin-mediated silica precipitation, the enzyme molecules become randomly co-entrapped in the newly formed silica material.<sup>32-33</sup>

Nevertheless, whereas the first method is not generally applicable, the latter methods lack control over silica morphology and properties as well as suffering from random and unspecific entrapment. Since R5 variants with different (posttranslational) modifications have been shown to trigger the formation of different silica materials,<sup>34</sup> their application in protein immobilisation would allow tailoring silica properties to individual proteins and applications. In addition, covalent linkage of the R5 peptide to the target protein should ensure an efficient and homogenous encapsulation of the protein within the silica material. However, access to such fusion proteins containing site-specifically modified R5 sequences by means of classic biological methods, such as bacterial expression, is severely limited. These limitations can be overcome by semisynthesis of protein-silaffin conjugates. Solid phase peptide synthesis enables the facile incorporation of modified amino acids at defined positions in a peptide sequence.<sup>35</sup> Subsequently, the modified peptide can be chemoselectively ligated to a recombinant protein, e.g. using the method of expressed protein ligation (EPL).<sup>36</sup> This method relies on the reaction between the N-terminal cysteine of one peptide or protein fragment with the C-terminal thioester of a second peptide or protein. The intermediate thioester spontaneously and irreversibly rearranges via a S→N acyl transfer resulting in a stable amide linkage of the two segments (Scheme 1).

Here EPL is used to generate stable conjugates between two selected target proteins (enhanced green fluorescent protein (eGFP) and thioredoxin (TRX)) and four R5 peptides. Such covalent protein-R5 conjugates serve two purposes: The covalent attachment of the silaffin R5 variants to the proteins ensures selective and efficient encapsulation of the protein in the silica matrix (Scheme 1). The difference to random entrapment in co-precipitation experiments is analysed. In addition, the specific

modifications of the R5 peptides will allow tailoring morphology and properties of the resulting silica material to requirements desired for specific proteins and/or applications.



**Scheme 1** General strategy for generation of protein-silaffin R5 conjugates using EPL and their auto-encapsulation during *in vitro* biomimetic silica formation (structure of human TRX in orange, PDB entry 1ERU<sup>37</sup>)

## Materials and methods

Detailed experimental procedures for the cloning and expression of protein constructs, characterisation of compounds with HPLC, mass spectrometry, scanning electron and fluorescence microscopy and the experiments for stability and activity of silica immobilised proteins are given in the electronic supplementary information (ESI†).

### Peptide synthesis

Peptides **A-D** (Table 1) were synthesised on solid phase using fluorenylmethoxycarbonyl (Fmoc-) chemistry and purified as described previously.<sup>34</sup>

### Expressed protein ligation

The recombinant eGFP-MESNa  $\alpha$ -thioester and peptides **A-D** were ligated to obtain four variants of semisynthetic eGFP-R5 conjugates. eGFP-MESNa thioester (250  $\mu$ M) and peptides **A-D** (1.25 mM) were dissolved in 100 mM Tris buffer at pH 8. Ethyl mercaptan (2 % v/v) was added and the reaction was incubated under shaking (350 rpm) for 20 h at room temperature. The reactions were monitored by SDS-PAGE and LC-MS analysis. Removal of excess peptide and exchange of buffer to 50 mM potassium phosphate pH 7 was achieved with ultrafiltration spin columns (MWCO 10K). Ligation of recombinant TRX-MESNa thioester (250  $\mu$ M) with peptides **A-D** (1.25 mM) was carried out in 100 mM Tris buffer pH 8 containing 5 mM TCEP and 1 % (v/v)

thiophenol. The reaction was shaken at 700 rpm and 30 °C for 24 h. Occurring precipitates were pelleted by centrifugation for 5 min at 14000 rpm. The supernatant was collected and buffer exchange and removal of excess peptide was achieved with Zeba Spin Desalting Columns (MWCO 7K). Ligation reactions were analysed by SDS-PAGE (8-16 % polyacrylamide gradient gel), LC-MS and HPLC. After concentration of protein solutions with ultrafiltration spin columns (MWCO 3K), protein concentrations were measured via UV-absorbance at 280 nm.

### 10 Silica precipitation assays

All silica precipitation assays were carried out in 50 mM potassium phosphate buffer at pH 7. Stock solutions of peptides **A-D**, proteins and protein-conjugates were prepared in 50 mM potassium phosphate buffer, pH 7. A solution of silicic acid was freshly generated from 250 mM tetramethoxysilane (TMOS) in 1 mM HCl for exactly 4 min before each assay. Precipitation of silica from solutions of silicic acid with peptides **A-D** was carried out as described previously.<sup>34</sup> Briefly, peptides were diluted in phosphate buffer to a final concentration of 470 μM. With addition of 25 mM silicic acid (final concentration), the silica precipitation reaction was initiated. After 30 min incubation at room temperature, silica precipitates were collected by centrifugation (5 min, 14000 rpm). The silica precipitates were washed twice with ddH<sub>2</sub>O. Silica precipitation assays using eGFP- and TRX-R5 conjugates, eGFP-OH and TRX-OH were carried out in exact the same manner using 470 μM of each protein. In Co-precipitation experiments, 470 μM eGFP-OH or TRX-OH were mixed with equimolar amounts of peptides **A-D** prior to initiation of silica precipitation by addition of silicic acid. Control experiments that were conducted without silicic acid or a R5 peptide variant in the reaction solution did not lead to formation of any precipitate. All assays were carried out at least in triplicate. The resulting silica material was analysed by fluorescence and scanning electron microscopy as described in the supplementary information (ESI†).

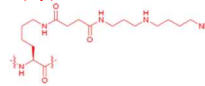
## Results and discussion

The strategy of silica immobilisation of proteins that are covalently linked to silaffin R5 peptides is demonstrated with two very different proteins, eGFP<sup>38</sup> and TRX.<sup>39</sup> The intrinsic fluorescence of the 28 kDa protein eGFP allows direct detection of protein localisation by microscopy as well as fast assessment of protein stability via its auto-fluorescence. Thioredoxins are 12 kDa proteins found in all kingdoms of life.<sup>39</sup> These enzymes reduce disulfide bonds in proteins by catalysing a cysteine thiol-disulfide exchange reaction and are involved in redox regulation and signaling of many important biological processes.<sup>40</sup> Thioredoxins are considered potentially valuable additives in food biotechnology since they are able to reduce disulfide bonds of allergens and thereby mitigate the allergenic response to wheat or increase the digestibility of milk.<sup>41,42</sup> In contrast to the cellular reducing agent glutathione, thioredoxins are also potent in reducing disulfide-containing venom neurotoxins thus rendering them inactive.<sup>43</sup> This suggests an application of thioredoxins as detoxifying agent or clinical antidote.

### eGFP and TRX-peptide conjugates

eGFP and TRX with a C-terminal sodium 2-mercaptoethanesulfonate (MESNa)-thioester moiety were generated by cleavage of the respective intein fusions proteins

60 **Table 1** Synthetic silaffin R5 peptides used in EPL

	Sequence	modification
<b>A</b>	CSSKKS <sup>GS</sup> YS <sup>GS</sup> GSK <sup>GSK</sup> RRIL	none
<b>B</b>	CSSKKS <sup>GS</sup> YS <sup>GS</sup> GK(Me) <sub>3</sub> GSKRRIL	K(Me) <sub>3</sub> = 
<b>C</b>	CSSK(Sp)KSGSYS <sup>GS</sup> GSK <sup>GSK</sup> (Sp)RRIL	K(Sp) = 
<b>D</b>	CSSKKS <sup>GS</sup> YS <sup>GS</sup> GSK <sup>Gp</sup> S <sup>K</sup> RRIL	pS = 

(Fig. S1 and Fig. S2†). The amino acids KFAEY (representing the native protein context of the Mxe GyrA intein) were C-terminally added to eGFP and TRX to ensure efficient intein cleavage (see ESI†).<sup>44</sup> The eGFP- and TRX-thioester proteins were linked to synthetic silaffin peptides **A-D**<sup>34</sup> carrying an N-terminal cysteine residue (Table 1) by expressed protein ligation.<sup>36</sup> Peptide **A** comprises the unmodified silaffin R5 sequence, peptide **B** contains a trimethylated lysine residue at position 13. In peptide **C**, the polyamine spermidine was attached to two lysine side chains and peptide **D** carries a single phosphoserine residue at position 15 in the peptide sequence (Table 1).

The cysteinyl peptides **A-D** were ligated to the eGFP- and TRX-MESNa thioester proteins in excellent yields (Table 2 and 3), all ligation reactions were analysed by SDS-PAGE (Fig. S3 and Fig. S8†) and the identity of all ligation products was confirmed by LC-MS analysis (Fig. S4-S7 and Fig. S9-S12†). The obtained eGFP- and TRX-silaffin conjugates were used for in vitro silica precipitation after excess peptides **A** to **D** from ligation reactions were removed by size exclusion chromatography or ultrafiltration to avoid any impact on silica precipitation.

### 85 Silica-precipitation with eGFP-peptide conjugates

Synthetic silaffin R5 peptide variants **A** to **D** have been shown to initiate precipitation of silica from a solution of silicic acid.<sup>34</sup> Moreover, the particular amino acid side chain modifications directly influence the morphology of the resulting silica precipitates. Whereas the unmodified R5 peptide **A** and peptide **B** with a trimethylated lysine induce formation of homogeneous spherical silica particles, peptide **C**, carrying two polyamine modifications, leads to silica particles with variable diameters (400–900 nm)<sup>34</sup> and a completely altered silica morphology, with clusters of nano-sized silica spheres, was observed with peptide **D**. All conjugates between eGFP and silaffin R5 variants **A-D** (Table 2) showed silica precipitation activity. The resulting silica precipitates (exhibiting an intense green color) were analysed by scanning electron (Fig. 1) and fluorescence microscopy (Fig. 2).

Cite this: DOI: 10.1039/c0xx00000x

www.rsc.org/xxxxxx

## ARTICLE TYPE

**Table 2** eGFP-peptide conjugates obtained by expressed protein ligation

Protein	+ Peptide	→ Conjugate	MW (calc.)	MW (obs.)	Ligation yield*
eGFP-MESNa	<b>A</b>	eGFP- <b>A</b>	29722 Da	29776 Da	80 %
	<b>B</b>	eGFP- <b>B</b>	29815 Da	29818 Da	66 %
	<b>C</b>	eGFP- <b>C</b>	30227 Da	30230 Da	68 %
	<b>D</b>	eGFP- <b>D</b>	29852 Da	29856 Da	69 %

\* Ligation yields were calculated from integrated peak areas of HPLC traces (Fig. S4-S7)

**Table 3** TRX-peptide conjugates obtained by expressed protein ligation

Protein	+ Peptide	→ Conjugate	MW (calc.)	MW (obs.)	Ligation yield*
TRX-MESNa	<b>A</b>	TRX- <b>A</b>	14688 Da	14684 Da	98 %
	<b>B</b>	TRX- <b>B</b>	14724 Da	14724 Da	91 %
	<b>C</b>	TRX- <b>C</b>	15143 Da	15139 Da	91 %
	<b>D</b>	TRX- <b>D</b>	14768 Da	14763 Da	95 %

\* Ligation yields were calculated based on integrated peak areas of HPLC traces (Fig. S9-S12)

Depending on which eGFP-peptide conjugate was used, distinct morphologies of the silica precipitates were observed, which share many features with particles obtained with peptides **A-D** only. eGFP-**A**, comprising the eGFP sequence and the unmodified R5-sequence, induces formation of homogenous spherical silica particles with diameters of approximately 1  $\mu\text{m}$  (Fig. 1a, Fig. S13, Table S1). Such spherical silica particles of homogenous size distribution were also observed with the unmodified peptide **A** alone. In that case, the average diameter was only 750 nm.<sup>34</sup> Using eGFP-**B**, spherical silica particles were obtained as well (Fig. 1b), but the average diameter (930 nm, Table S1) is slightly decreased when compared to particles resulting from eGFP-**A**. These results correlate well with the silica particles derived from peptide **B** with a trimethylated lysine residue. The R5 peptide variant with spermidine units attached to two lysine side chains (peptide **C**) induces the formation of spherical silica particles with a rather inhomogeneous size distribution. The silica material resulting from the eGFP-**C** conjugate seems to be composed of highly connected small spherical silica particles (Fig. 1c). This silica morphology does not much resemble the silica spheres with variable size distribution observed using peptide **C** alone and it distinctly differs from the large, homogenous silica spheres obtained with eGFP-**A** and **B** conjugates. Also the eGFP-**D** conjugate, containing the R5 peptide with the single phosphoserine residue, leads to more heterogeneous silica material. The silica precipitate appears to be composed of nanometer-sized silica particles aggregating into clusters of larger spheres (Fig. 1d). Similar fuzzy silica material was observed with peptide **D** and is assumed to arise from electrostatic interactions of the phosphate group with the silicic acid and silica during the process of silica formation.<sup>34</sup> Remarkably, this effect of the phosphate group is still very pronounced even if the short peptide **D** (2.2 kDa) is coupled to the much larger eGFP (27.6 kDa).

The intrinsic fluorescence of eGFP allowed analysis by

fluorescence microscopy (Fig. 2) and all silica particles showed a bright green fluorescence. No background fluorescence outside the silica material was observed (Fig. S15<sup>†</sup>). Silica particles derived from R5 peptides only showed no intrinsic fluorescence (data not shown). Therefore, eGFP could be clearly localized within or at least tightly associated to the silica material (Fig. S15<sup>†</sup>). Together electron and fluorescence microscopic analysis of the silica materials obtained with eGFP-peptide conjugates indicates that covalent attachment of silaffin peptides **A-D** to eGFP results in specific and homogenous incorporation of the protein into the silica material (Fig. 1 and Fig. 2, a-d).

Co-precipitation experiments of eGFP and R5 peptides **A-D** in which both components were simply mixed in equimolar amounts in phosphate buffer resulted in silica precipitation upon addition of silicic acid. Here eGFP and peptides were not covalently linked and an eGFP variant with a free carboxyl group at the C-terminus was used to avoid in situ ligation reactions with R5 peptides. The resulting silica precipitates were also analysed by electron and fluorescence microscopy (Fig. 1 and Fig. 2, e-h). The electron micrographs show rather unstructured silica materials. In silica material resulting from co-precipitation of eGFP with peptide **A** and **C**, spherical silica particles started to form, as observed with peptides **A** and **C** only (Fig. 1, e and g). In contrast, co-precipitation of eGFP with peptides **B** and **D** leads to unstructured silica material with nanometer-sized substructures (Fig. 1, f and h).

Fluorescence micrographs of these silica materials show a broad distribution of eGFP fluorescence, indicating that eGFP is associated with the silica (Fig. 2, e-h, Fig. S16). However, the protein seems to be rather randomly distributed over the silica material and not specifically entrapped. We surmise that the peptides **A-D** initiate polycondensation of silicic acid in the co-precipitation mixture and that during this silica formation process eGFP precipitates and becomes randomly entrapped. The presence of eGFP in the co-precipitation mixture interferes with

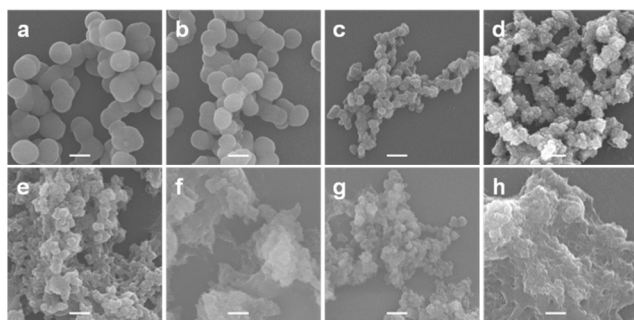


**Fig. 1** Scanning electron micrographs of silica particles resulting from silica precipitations with covalent eGFP-peptide conjugates (a-d) and from silica co-precipitation with eGFP and peptide variants (e-h). Scale bars 1  $\mu\text{m}$ . a) eGFP-A conjugate; b) eGFP-B conjugate; c) eGFP-C conjugate; d) eGFP-D conjugate; e) co-precipitation with eGFP and peptide A; f) co-precipitation with eGFP and peptide B; g) co-precipitation with eGFP and peptide C; h) co-precipitation with eGFP and peptide D.

silica precipitation activity of all peptide variants. Control experiments revealed that eGFP itself induces amorphous precipitation of silica from a solution of silicic acid and becomes associated with the silica during this process (Fig. S17<sup>†</sup>). Therefore no quantitative comparison of silica precipitation and eGFP incorporation between both conditions was possible.

Immobilisation of eGFP in a silica matrix is aimed to result in stabilisation of the protein as described previously for other immobilisation strategies.<sup>27,48</sup> We analysed the stabilisation of silica entrapped eGFP based on sodium dodecyl sulfate (SDS) induced denaturation linked to the decrease of intrinsic fluorescence (see ESI<sup>†</sup>).<sup>49,50</sup> Compared to soluble eGFP, silica immobilised eGFP is greatly stabilised and retains between 50 and 90% of its initial fluorescence intensity after treatment with SDS depending on the R5 peptide used. Soluble eGFP only retains a maximum of 10% fluorescence (Fig. S18<sup>†</sup>). Obviously a smaller fraction of immobilised eGFP remains sensitive to denaturants such as SDS whereas the major fraction is stabilised by being tightly enclosed in silica.

### 30 Silica-precipitation with TRX-peptide conjugates

Covalent conjugates of TRX and peptide variants A to D were obtained by quantitative EPL reactions (Table 3, Fig. S8<sup>†</sup>). According to the TRX crystal structure the carboxy-terminus is not involved in secondary structure formation and easily accessible.<sup>51</sup> The additional amino acids KFAEY representing the native protein context of the *Mxe* GyrA intein at the C-terminus of the TRX sequence to ensure proper intein cleavage<sup>44</sup> result in a stable and flexible attachment of the R5 peptides to TRX. Excess peptides and ligation additives such as thiophenol were removed from the crude ligation mixtures prior to silica precipitation experiments. The morphologies of the resulting silica precipitates were investigated with scanning electron microscopy (Fig. 3). All TRX-peptide conjugates were able to initiate precipitation of silica from a solution of silicic acid. The TRX-A conjugate induced the formation of large silica spheres with diameters exceeding 1  $\mu\text{m}$  (Fig. 3a, Fig. S14<sup>†</sup>). Silica particles resulting from TRX-B present a much more narrow size distribution (Fig. 3b, Fig. S14<sup>†</sup>). This silica morphology correlates well with silica

particles

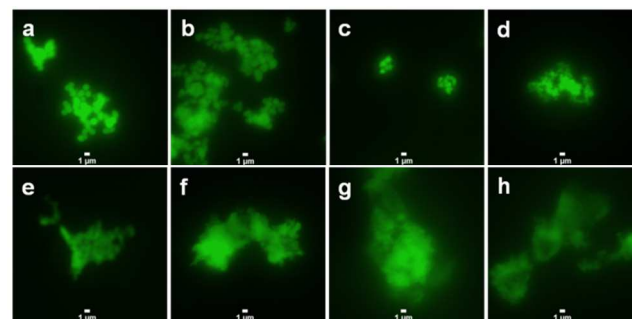


**Fig. 2** Fluorescence micrographs of silica particles resulting from silica precipitations with covalent eGFP-peptide conjugates (a-d) and from silica co-precipitation with eGFP and peptide variants (e-h). Scale bars 1  $\mu\text{m}$ . a) eGFP-A conjugate; b) eGFP-B conjugate; c) eGFP-C conjugate; d) eGFP-D conjugate; e) co-precipitation with eGFP and peptide A; f) co-precipitation with eGFP and peptide B; g) co-precipitation with eGFP and peptide C; h) co-precipitation with eGFP and peptide D.

obtained from peptide B carrying the trimethylated lysine residue.<sup>34</sup>

Similar to the inhomogeneous silica spheres resulting from peptide C (spermidine modification), the TRX-C conjugate induces formation of spherical silica particles with an inhomogeneous size distribution (Fig. 3c). The single phosphoserine residue in peptide D influences silica formation most dramatically. The silica material resulting from peptide D appeared to be composed of small, nanometer-sized silica spheres.<sup>34</sup> With the TRX-D conjugate, spherical silica particles were observed (Fig. 3d). However, the single particles are not as well-defined as observed for the other TRX-peptide conjugates. The morphology of this silica material clearly differs from silica obtained with peptide D or with the eGFP-D conjugate (Fig. 1).

Here a quantitative comparison of the amount of precipitated silica was possible since TRX does not significantly influence silica precipitation. Specific silica precipitation activities of all TRX-peptide conjugates were in the same range as observed for unmodified peptide A ( $0.71 \pm 0.02$  pmol Si/nmol peptide\*min, Table 4). Hence the covalent conjugation of a 5fold larger protein to the R5 peptide does not interfere with its silica precipitation activity.

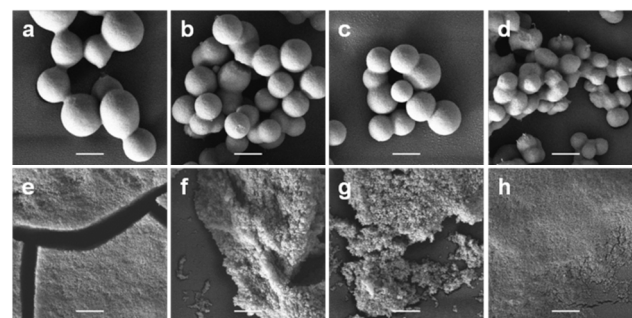


**Fig. 3** Scanning electron micrographs of silica particles resulting from silica precipitations with covalent TRX-peptide conjugates (a-d) and from silica co-precipitation with TRX and peptide variants (e-h). Scale bars 1  $\mu\text{m}$ . a) TRX-A conjugate; b) TRX-B conjugate; c) TRX-C conjugate; d) TRX-D conjugate; e) co-precipitation with TRX and peptide A; f) co-precipitation with TRX and peptide B; g) co-precipitation with TRX and peptide C; h) co-precipitation with TRX and peptide D.

Cite this: DOI: 10.1039/c0xx00000x

www.rsc.org/xxxxxx

## ARTICLE TYPE

**Table 4** Characteristics of silica precipitation with TRX-peptide conjugates and co-precipitation of TRX with peptides **A** to **D**

	Specific activity <sup>a</sup>	Loading of silica with TRX or conjugate <sup>b</sup>	Loading efficiency <sup>c</sup>
TRX- <b>A</b>	0.76 ± 0.02	16.8 ± 2.4	37.5 ± 5.4 %
TRX- <b>B</b>	0.71 ± 0.01	12.3 ± 0.4	26.5 ± 0.8 %
TRX- <b>C</b>	0.69 ± 0.06	14.3 ± 0.3	31.3 ± 0.7 %
TRX- <b>D</b>	0.82 ± 0.12	15.3 ± 1.5	33.5 ± 3.4 %
TRX + <b>A</b> (Co-precipitation)	0.54 ± 0.03	8.8 ± 1.0	16.8 ± 2.0 %
TRX + <b>B</b> (Co-precipitation)	0.65 ± 0.03	13.1 ± 0.3	28.8 ± 0.6 %
TRX + <b>C</b> (Co-precipitation)	0.54 ± 0.01	9.1 ± 0.1	17.0 ± 0.3 %
TRX + <b>D</b> (Co-precipitation)	0.46 ± 0.03	4.1 ± 0.8	6.8 ± 1.3 %

<sup>a</sup> specific silica precipitation activity at pH 7.0 given in pmol silicon per min and nmol peptide or TRX-peptide conjugate; <sup>b</sup> given in (nmol) protein/(nmol) SiO<sub>2</sub>; <sup>c</sup> (nmol protein in nanoparticles/nmol protein used initially for silica precipitation) \* 100.

Co-precipitation experiments with TRX and peptides **A** to **D** in equimolar ratios, similar to those described above for eGFP, were also carried out and led to silica formation in all cases (Fig. 3, e-h). To ensure that no *in situ* ligation occurred during silica precipitation, the TRX C-terminal thioester moiety was previously hydrolysed by treatment with dithiothreitol (DTT, Fig. S19†). Most silica precipitates are composed of small silica nanospheres or amorphous silica, but no larger silica spheres were observed. The silica material resulting from co-precipitation of TRX with peptides **A** to **D** represents the small silica spheres occurring in the early stage of the silica precipitation process and in contrast to eGFP, TRX shows no silica precipitating activity by itself but it inhibits peptides **A-D** in their normal precipitation activity since the typical μm-sized silica spheres are not formed (Fig. 3, e-h). During co-precipitation with TRX, peptides **A-D** also show a markedly reduced specific silica precipitation activity in comparison to peptides **A-D**<sup>34</sup> or the respective TRX-peptide conjugates (Table 4). The presence of TRX in co-precipitation assays not only alters the morphology of the silica material obtained but it also reduces the amount of precipitated silica. Covalently attached TRX, however, does not influence the silica precipitation of peptides **A-D** in terms of amount and morphology of resulting silica material (Fig. 3, a-d, Table 4).

Entrapment of TRX in silica particles could not be verified as easily as for eGFP by fluorescence microscopy. Loading of silica material with TRX and TRX-peptide conjugates was determined by dissolution of silica and subsequent analysis of the protein content with HPLC (see ESI for detailed procedures†). The absolute amount of protein content in the silica material is also important as a reference for determining activity of silica encapsulated enzymes.

The R5 peptides co-precipitate during silica formation and become entrapped within the silica material.<sup>23,52,53</sup> Using peptide **A**, typically 32.7 ± 2.1 % of peptide initially used for silica precipitation become entrapped within the silica particles.<sup>52</sup> In total 16.8 ± 1.1 nmol of peptide **A** are loaded per nmol of precipitated SiO<sub>2</sub>. Silica precipitation with the covalently linked TRX-peptide conjugates resulted in comparable amounts of encapsulated proteins (Table 4). During silica formation with

TRX-peptide conjugates, about one third of the initially supplied conjugate becomes entrapped, except for TRX-**B**. This conjugate containing the trimethylated lysine residue shows slightly decreased encapsulation efficiency compared to the other conjugates despite exhibiting similar silica precipitation activity (Table 4). This effect might be due to the permanent positive charge arising from the trimethylated lysine that impairs association with the newly formed silica by electrostatic repulsion. In cases when TRX was not covalently linked to peptides **A**, **C** and **D**, distinctly decreased amounts of TRX were encapsulated in the silica material. However, similar amounts of TRX were encapsulated using TRX-**B** conjugate or co-precipitation of TRX with peptide **B** (Table 4). During co-precipitation of TRX and peptide **A**, with 8.8 ± 1.0 nmol/nmol SiO<sub>2</sub> (16.8 ± 2.0 %), only half as much of TRX became associated with the silica when compared to the TRX-**A** conjugate. A similar behaviour was observed for TRX-**C** and TRX-**D**. Only TRX-**B** gave similar values for the covalent and the co-precipitation approach, emphasizing the special role of the trimethyl lysine residue. The lowest amount of TRX was encapsulated in silica when the protein was co-precipitated in presence of peptide **D**: With 4.1 ± 0.8 nmol/nmol SiO<sub>2</sub>, only 6.8 ± 1.3 % of TRX from the reaction solution was trapped in the silica material.

These results prove that a highly efficient encapsulation of target proteins in silica can be achieved by covalent attachment to the R5 peptide **A** and its variants **C** and **D**. However, R5 peptide-driven silica immobilisation also depends on the nature of the protein used. There are several examples in the literature demonstrating successful co-precipitation of enzymes but a large molar excess of R5 peptide is needed in order to achieve high yields of immobilisation.<sup>32,33</sup> In contrast, covalent protein-R5 conjugates lead to efficient protein encapsulation with equimolar amounts of protein and R5 peptide.<sup>29</sup>

#### Release of TRX and TRX-peptide conjugates from silica material

The silica entrapped proteins and peptides are not covalently bound but associate to silica material based on electrostatic

interactions and hydrogen bonding between peptide side chains and silanol groups. The R5 peptide has been shown to be partly

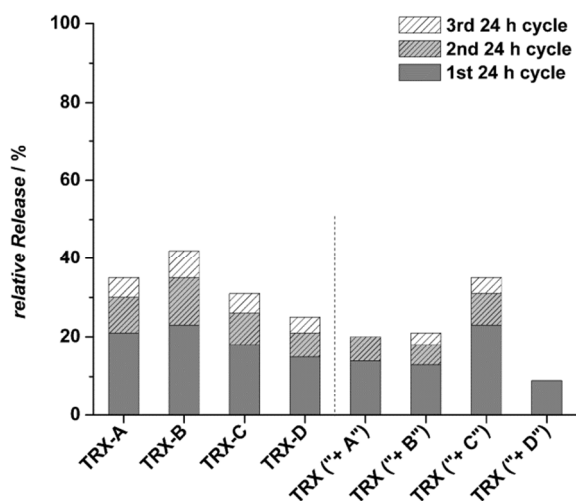


**Fig. 4** Release of TRX-peptide conjugates and TRX from silica material after incubation in PBS for 3 days (24 hour measurement cycles).

Percentages are based on the total amount of TRX encapsulated. The labels TRX-A, TRX-B, TRX-C and TRX-D represent the corresponding conjugates, TRX ("+ X") marks the co-precipitation experiments with different peptides.

released from silica depending on pH and buffer conditions.<sup>52</sup> In other approaches of hybrid silica formation with bioactive molecules, uncontrolled, diffusion-based release of an encapsulated antimicrobial peptide or apoptotic protein from silica materials was observed.<sup>54,55</sup> Here it is analysed if TRX is permanently entrapped in the silica or if the protein is gradually released from silica by suspending silica materials in PBS buffer and incubation at 37°C over a period of 3 days. After each day, the supernatant was separated from the silica material and analysed for protein content by HPLC. The silica material was re-suspended in fresh PBS buffer for the next 24 h cycle.

The highest rate of protein release is observed during the first 24 h for all TRX-silica hybrid materials (Fig. 4, Table S3†). In the second and third 24 hour cycles considerably less protein leaks from the silica material or, in two cases, no release can be detected any more. Comparison of the TRX-peptide (A-D) conjugates reveals a slightly increased release of TRX-B with 42% of the TRX-B conjugate being washed out after 3 days (compared to the initial loading, Fig. 4). TRX-B carries a permanent positive charge that might impair electrostatic interactions and hydrogen bonding between the protein conjugate and the silica material and therefore causes a reduced affinity of TRX-B to the silica.

The lowest amount of released protein was observed for the phosphorylated peptide D, both from silica obtained with TRX-D or by co-precipitation of TRX and peptide D (Fig. 4; Table S3†). The single phosphoserine residue in peptide D also influenced the morphology of silica precipitates most severely and the clusters of small silica-nanospheres might contribute to a tight entrapment of TRX in the silica material (Fig. 4). From all silica materials analysed, less than half of the initially encapsulated TRX-peptide conjugates or TRX is released even after three day incubation in

PBS buffer at 37 °C (Fig. 4).

### Activity of silica immobilised TRX

Thioredoxins are the major cellular protein disulfide isomerases and contain a dithiol/disulfide active site (CGPC). *In vivo*, the cysteine disulfide of TRX is reduced to the dithiol form by electrons from NADPH via a thioredoxin reductase.<sup>39</sup> An elegant *in vitro* assay for thioredoxin activity is based on the reduction of insulin catalysed by thioredoxin in the presence of DTT.<sup>56</sup> The disulfide in the CGPC active site motif of TRX (TRX-S2) is rapidly reduced by DTT resulting in free sulfhydryl groups

**Table 5** Specific activity of TRX and silica immobilised TRX in reduction of insulin

	Spec. activity <sup>a</sup>
TRX-MESNa thioester	$1.6 \times 10^{-3}$
TRX-OH	$1.5 \times 10^{-3}$
TRX-A conjugate	$1.2 \times 10^{-3}$
TRX-B conjugate	$1.0 \times 10^{-3}$
TRX-C conjugate	$0.7 \times 10^{-3}$
TRX-D conjugate	$0.9 \times 10^{-3}$
Silica immobilised TRX-A conjugate	$2.4 \times 10^{-3}$
Silica immobilised TRX-B conjugate	$2.7 \times 10^{-3}$
Silica immobilised TRX-C conjugate	$1.3 \times 10^{-3}$
Silica immobilised TRX-D conjugate	$3.0 \times 10^{-3}$
Silica immobilised TRX, co-precipitated with peptide A	$0.9 \times 10^{-3}$
Silica immobilised TRX, co-precipitated with peptide B	$1.0 \times 10^{-3}$
Silica immobilised TRX, co-precipitated with peptide C	$0.7 \times 10^{-3}$
Silica immobilised TRX, co-precipitated with peptide D	$0.6 \times 10^{-3}$

<sup>a</sup> calculated as  $\Delta A_{650} \times \text{min}^{-1}$  in the linear range of increase of absorption /  $\mu\text{g}$  protein.

(TRX-(SH)<sub>2</sub>). Subsequently, TRX-(SH)<sub>2</sub> catalyses a thiol-disulfide exchange reaction with insulin (Scheme S1†). Reduction of the interchain disulfide bonds of insulin results in the precipitation of the insulin B chain. The rate of insulin reduction can be monitored as the increase of turbidity at 650 nm caused by insulin B chain aggregation.<sup>57</sup> Notably, DTT does not cause detectable reduction of insulin and precipitation of the B chain within 20 min (Fig. 5a). However, insulin reduction by DTT followed by aggregation of the B chain could be observed at prolonged incubation times. Therefore, all measurements for determination of TRX activity were limited to 20 min.

The TRX variants with a MESNa thioester moiety (TRX-MESNa) or with an  $\alpha$ -carboxyl group at the C-terminus (TRX-OH) both showed similar activity (Fig. 5a, Table 5). For the TRX-MESNa thioester, turbidity could typically be observed after a delay time of 2 min. With TRX-OH, precipitation of insulin B chain was detected after a much shorter delay time since TRX-OH was obtained by treatment of the TRX-MESNa with an excess of DTT to hydrolyse the C-terminal thioester moiety. Thus, TRX-OH was already fully reduced and did not require initial activation. Chemoselective ligation of the differently modified silaffin peptides A to D to the C-terminus of TRX via expressed protein ligation only slightly affects its enzymatic activity (Fig. 5a, Table 5). Besides a generally reduced relative specific activity (given as  $\Delta A_{650} \times \text{min}^{-1}/\mu\text{g}$  protein) of the TRX-peptide conjugates in comparison to the TRX-MESNa thioester and TRX-OH protein, also a distinct difference between the individual conjugates became apparent. The conjugates TRX-

A comprising the unmodified silaffin R5 peptide A or TRX-B containing peptide B with the trimethylated lysine residue

showed highest activity in insulin reduction among the

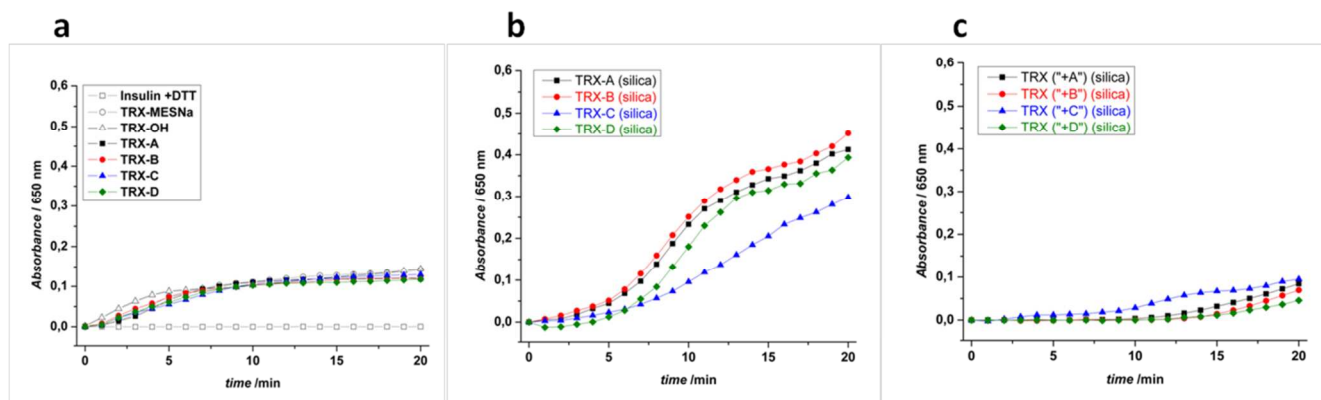


**Fig. 5** Activity of TRX and silica immobilised TRX in reduction of insulin by DTT. **a)** Activity of TRX with C-terminal MESNa thioester moiety (grey circles), TRX with free carboxyl group (grey triangles) and TRX-peptide conjugates: TRX-A (black squares), TRX-B (red circles), TRX-C (blue triangle) and TRX-D (green rhombus). DTT did not cause reduction of insulin (grey circles). **b)** Activity of silica immobilised TRX-peptide conjugates: Silica-immobilised TRX-A (black squares), Silica-immobilised TRX-B (red circles), Silica-immobilised TRX-C (blue triangles) and Silica-immobilised TRX-D (green rhombus). **c)** Activity of silica immobilised TRX after co-precipitation during silica formation with different peptides: TRX immobilised in silica resulting from peptide A (black squares), TRX immobilised in silica resulting from peptide B (red circles), TRX immobilised in silica resulting from peptide C (blue triangles) and TRX immobilised in silica resulting from peptide D (green rhombus).

conjugates. In contrast, the spermidine-modification in TRX-C and the phosphoserine residue in TRX-D had a more pronounced negative impact on enzymatic activity (Table 5).

TRX activity was observed for all variants after silaffin-mediated immobilisation (Fig. 5, Table 5) but a delay in insulin precipitation was found in comparison to soluble TRX and TRX-conjugates (Fig. 5a and 5b). This delay is most likely caused by restricted diffusion within the porous silica material. Since the activator DTT is relatively small, we surmise that diffusion and precipitation of reduced insulin chains are responsible for the delay. For the silica immobilised TRX-conjugates insulin B chain precipitation could be observed after 5 to 7 min (Table S4†). This prolonged delay time was followed by high rates of insulin reduction detected as  $\Delta A_{650} \times \text{min}^{-1}$  by silica encapsulated TRX-peptide conjugates. Least active among the silica immobilised TRX-silaffin conjugates was silica immobilised TRX-C (Table 5). Also TRX-C conjugate in buffer showed decreased enzymatic activity compared to the other TRX-peptide conjugates (Table 5) hinting towards a negative influence of the two spermidine modifications in peptide C on TRX activity.

If TRX was immobilised in silica by co-precipitation with the differently modified silaffin peptides, distinctly altered silica morphologies were obtained (Fig. 3). Also distinctly less protein became entrapped in the silica material during the co-precipitation process (Table 4). Nevertheless, to ensure comparability of enzymatic activities, a respective amount of silica with co-precipitated TRX based on the loading of silica with TRX (Table 4) was used for activity assays.

Activity of co-precipitated TRX could only be observed after much longer delay times (Fig. 5c), which supports our argument that diffusion within the silica material limits this process. Precipitation of the insulin B chain by TRX co-precipitated with peptides A, B and D became visible only after 12-15 min (Table S4†). This suggests that longer times are needed until substrate finds entrapped TRX in the silica material. However, we cannot exclude that TRX is partially inactivated during silica

precipitation. Only for TRX co-precipitated with peptide C shorter delay times could be detected (Fig. 5c), which can be explained with the increased release of TRX from this silica material described above (Fig. 4). In all assays enzymatic activity of TRX was monitored for 20 min only to prevent direct reduction of insulin by DTT (see ESI†).

Overall, TRX-silaffin conjugates provide a more efficient and homogenous encapsulation of the target proteins in combination with improved enzymatic activities and/or accessibility. Systematic investigations of protein release and enzymatic activity of encapsulated proteins revealed a clear influence of the differently modified silaffin peptides, which allows tuning of silica properties to specific requirements in different applications by the choice of silaffin peptides. Even hybrid protein-silica materials that can be developed into systems for sustained release of proteins from silica or into efficient biocatalysts, especially when introducing more complex modification patterns as found in native silaffins can be envisioned.

## Conclusion

Silaffin peptides are powerful tools for efficient silica formation under mild conditions and several strategies for enzyme immobilisation using silaffins were already reported.<sup>29-33</sup> In combination with expressed protein ligation stable conjugates made of expressed target proteins and synthetic, modified silaffin peptides can be efficiently generated. Almost quantitative ligation yields provide easy access to the required modified proteins for immobilisation. Here the highly efficient and homogenous encapsulation of two functional proteins, eGFP and thioredoxin, in silica material was achieved. Different morphologies of the obtained silica materials depend on the nature of silaffin peptides used and result in different protein release rates as well as activities. If eGFP or TRX were not covalently linked to the silaffin variants, random and less efficient co-precipitation of the

proteins during silica formation was observed also leading to lower activities.

These findings provide a rational basis for the development of modified silaffin peptides into efficient agents for controlled silica precipitation and the biocompatible encapsulation of proteins. Silica material properties can be tailored to the requirements of a given enzyme in order to achieve reasonable stabilisation and activity for the desired applications such as controlled release vehicles or stable biocatalysts.

## Acknowledgements

The authors gratefully acknowledge the Faculty Center for Nanostructure Research at the University of Vienna and Stephan Puchegger for help with electron microscopy. We thank Katja Bäumel and Manuel Felkl for excellent technical assistance. Financial support from the Institute of Silicon Chemistry at the Technische Universität München and Wacker Chemie AG is gratefully acknowledged.

## Notes and references

<sup>a</sup> University of Vienna, Department of Chemistry, Institute of Biological Chemistry, Währinger Straße 38, 1090 Vienna, Austria. Fax: +43 14277 9705; Tel: +43 14277 70501; E-mail: christian.becker@univie.ac.at

<sup>b</sup> present address: Ecole polytechnique Fédérale de Lausanne, Fondation Sandoz Chair in Biophysical Chemistry of Macromolecules, 1015 Lausanne, Switzerland.

† Electronic Supplementary Information (ESI) available: Detailed experimental methods, HPLC and mass spectrometry analyses of protein thioesters and protein-silaffin conjugates. See DOI: 10.1039/b000000x/

- 1 U. T. Bornscheuer, *Angew. Chem. Int. Ed.* 2003, **42**, 3336.
- 2 D. N. Tran, K. J. Balkus Jr, *Acs Catal.* 2011, **1**, 956.
- 3 C. T. Kresge, M. E. Leonowicz, W. J. Roth, J. C. Vartuli, J. S. Beck, *Nature* 1992, **359**, 710.
- 4 Y. Wan, D. Zhao, *Chem. Rev.* 2007, **107**, 2821.
- 5 K. C. W. Wu, Y. Yamauchi, *Mater. Chem.* 2012, **22**, 1251.
- 6 J. F. Diaz, K. J. J. Balkus Jr, *Mol. Catal. B: Enzym.* 1996, **2**, 115.
- 7 T. L. Simpson, B. E. Volcani, *Silicon and Siliceous Structures in Biological Systems*, Springer:New York, 1981.
- 8 L. De Stefano, A. Lamberti, L. Rotiroli, M. De Stefano, *Acta Biomater.* 2008, **4**, 126.
- 9 H. E. Townley, A. R. Parker, H. White-Cooper, *Adv. Funct. Mater.* 2008, **18**, 369.
- 10 D. K. Gale, T. Gutu, J. Jiao, C. H. Chang, G. L. Rorrer, *Adv. Funct. Mater.* 2009, **19**, 926.
- 11 M. S. Aw, S. Simovic, J. Addai-Mensah, D. Losic, *Nanomedicine* 2011, **6**, 1159.
- 12 M. Bariana, M. S. Aw, M. Kurkuri, D. Losic, *Int. J. Pharm.* 2013, **443**, 230.
- 13 E. Brunner, P. Richthammer, H. Ehrlich, S. Paasch, S. Ueberlein, K. H. van Pee, *Angew. Chem. Int. Ed.* 2009, **48**, 9724.
- 14 N. Kröger, R. Deutzmann, C. Bergsdorf, M. Sumper, *Proc. Natl. Acad. Sci. U. S. A* 2000, **97**, 14133.
- 15 M. Sumper, E. Brunner, G. Lehmann, *FEBS Lett.* 2005, **579**, 3765.
- 16 N. Kröger, C. Bergsdorf, M. Sumper, *EMBO J.* 1994, **13**, 4676.
- 17 N. Kröger, C. Bergsdorf, M. Sumper, *Eur. J. Biochem.* 1996, **239**, 259.
- 18 N. Kröger, G. Lehmann, R. Rachel, M. Sumper, *Eur. J. Biochem.* 1997, **250**, 99.
- 19 N. Kröger, R. Wetherbee, *Protist* 2000, 151, 263.
- 20 S. Wenzl, R. Hett, P. Richthammer, M. Sumper, *Angew. Chem. Int. Ed.* 2008, **47**, 1729.
- 21 P. Richthammer, M. Börmel, E. Brunner, K. H. van Pee, *ChemBioChem*, 2011, **12**, 1362.
- 22 A. Scheffel, N. Poulsen, S. Shian, N. Kröger, *Proc. Natl. Acad. Sci. U. S. A.* 2011, **108**, 3175.
- 23 N. Kröger, R. Deutzmann, M. Sumper, *Science* 1999, **286**, 1129.
- 24 N. Kröger, R. Deutzmann, M. Sumper, *J. Biol. Chem.* 2001, **276**, 26066.
- 25 N. Kröger, S. Lorenz, E. Brunner, M. Sumper, *Science* 2002, **298**, 584.
- 26 C. C. Lechner, C. F. W. Becker, *J. Pept. Sci.* 2014, **20**, 152.
- 27 N. Poulsen, C. Berne, J. Spain, N. Kröger, *Angew. Chem. Int. Ed.* 2007, **46**, 1843.
- 28 V. C. Sheppard, A. Scheffel, N. Poulsen, N. Kröger, *Appl. Environ. Microbiol.* 2012, **78**, 211.
- 29 D. H. Nam, K. Won, Y. H. Kim, B. I. Sang, *Biotechnol. Progr.* 2009, **25**, 1643.
- 30 W. D. Marner, A. S. Shaikh, S. J. Muller, J. D. Keasling, *Biotechnol. Progr.* 2009, **25**, 417.
- 31 O. Choi, B. C. Kim, J. H. An, K. Min, Y. H. Kim, Y. Um, M. K. Oh, B. I. Sang, *Enzyme Microb. Technol.* 2011, **49**, 441.
- 32 H. R. Luckarift, J. C. Spain, R. R. Naik, M. O. Stone, *Nat. Biotechnol.* 2004, **22**, 211.
- 33 R. R. Naik, M. M. Tomczak, H. R. Luckarift, J. C. Spain, M. O. Stone, *Chem. Commun.* 2004, **15**, 1684.
- 34 C. C. Lechner, C. F. W. Becker, *Chem. Sci.* 2012, **3**, 3500.
- 35 R. B. Merrifield, *J. Am. Chem. Soc.* 1963, **85**, 2149.
- 36 T. W. Muir, D. Sondhi, P. A. Cole, *Proc. Natl. Acad. Sci. U. S. A.* 1998, **95**, 6705.
- 37 A. Weichsel, J. R. Gasdaska, G. Powis, W. R. Montfort, *Structure* 1996, **4**, 735.
- 38 T. T. Yang, L. Cheng, S. R. Kain, *Nucleic Acids Res.* 1996, **24**, 4592.
- 39 A. Holmgren, *Annu. Rev. Biochem.* 1985, **54**, 237.
- 40 E. S. Arnér, A. Holmgren, *Eur. J. Biochem.* 2000, **267**, 6102.
- 41 B. B. Buchanan, C. Adamidi, R. M. Lozano, B. C. Yee, M. Momma, K. Kobrehel, M. Ermel, O. L. Frick, *Proc. Natl. Acad. Sci. U. S. A.* 1997, **94**, 5372.
- 42 G. del Val, B. C. Yee, R. M. Lozano, B. B. Buchanan, R. W. Ermel, Y. M. Lee, O. L. Frick, *J. Allergy Clin. Immunol.* 1999, **103**, 690.
- 43 R. M. Lozano, B. C. Yee, B. B. Buchanan, *Arch. Biochem. Biophys.* 1994, **309**, 356.
- 44 M. W. Southworth, K. Amaya, T. C. Evans, M. Q. Xu, F. B. Perler, *Biotechniques* 1999, **27**, 110.
- 45 D. C. Prasher, V. K. Eckenrode, W. W. Ward, F. G. Prendergast, M. J. Cormier, *Gene* 1992, **111**, 229.
- 46 M. Ormö, A. B. Cubitt, K. Kallio, L. A. Gross, R. Y. Tsien, S. J. Remington, *Science* 1996, **273**, 1392.
- 47 F. Yang, L. G. Moss, G. N. J. Phillips, *Nat. Biotechnol.* 1996, **14**, 1246.
- 48 A. Cao, Z. Ye, Z. Cai, E. Dong, X. Yang, G. Liu, X. Deng, Y. Wang, S. T. Yang, F. Wang, M. Wu, Y. Liu, *Angew. Chem. Int. Ed.* 2010, **49**, 3022.
- 49 K. M. Alkaabi, A. Yafea, S. S. Ashraf, *Appl. Biochem. Biotechnol.* 2005, **126**, 149.
- 50 S. H. Bokman, W. W. Ward, *Biochem. Biophys. Res. Commun.* 1981, **101**, 1372.
- 51 S. K. Katti, D. M. LeMaster, H. J. Eklund, *Mol. Biol.* 1990, **212**, 167.
- 52 C. C. Lechner, C. F. W. Becker, *Bioorg. Med. Chem.* 2013, **21**, 3533.
- 53 M. R. Knecht, D. W. Wright, *Chem. Commun.* 2003, **24**, 3038.
- 54 D. Eby, K. E. Farrington, G. R. Johnson, *Biomacromolecules* 2008, **9**, 2487.
- 55 K. I. Sano, T. Minamisawa, K. Shiba, *Langmuir* 2010, **26**, 2231.
- 56 A. Holmgren, *J. Biol. Chem.* 1979, **254**, 9627.
- 57 F. Sanger, *Biochem. J.* 1949, **44**, 126.

## Graphical Abstract for

## Immobilizing proteins on silica with site-specifically attached modified silaffin peptides

Site-specific modification of proteins with synthetic silaffin peptides allows efficient encapsulation in biomimetic silica particle. Variations in silaffin modifications provide control over particle shape, protein load and activity.

